arXiv:cond-mat/9402018v1 4 Feb 1994

FINITE-SIZE SCALING STUDIES OF REACTION-DIFFUSION SYSTEMS

Part II: Open Boundary Conditions

Haye Hinrichsen[†], Klaus Krebs[‡], Markus Pfannmüller[‡] and Birgit Wehefritz[‡]

[†] *Freie Universität Berlin, Fachbereich Physik*
Arnimallee 14, D-14195 Berlin, Germany

[‡] *Universität Bonn, Physikalisches Institut*
Nußallee 12, D-53115 Bonn, Germany

Abstract

We consider the coagulation-decoagulation model on an one-dimensional lattice of length L with open boundary conditions. Based on the empty interval approach the time evolution is described by a system of $\frac{L(L+1)}{2}$ differential equations which is solved analytically. An exact expression for the concentration is derived and its finite-size scaling behaviour is investigated. The scaling function is found to be independent of initial conditions. The scaling function and the correction function for open boundary conditions are different from those for periodic boundary conditions.

Key words: Reaction-diffusion systems, finite-size scaling, non-equilibrium statistical mechanics, coagulation model

PACS numbers: 05.40.+j, 05.70.Ln, 82.20.Mj

BONN HE-94-01
cond-mat/9402018
Bonn University
January 1994
ISSN-0172-8733

1 Introduction

In this article we continue the investigation of the finite-size scaling properties of reaction-diffusion models defined on an one-dimensional lattice of L sites. We consider the example of a special model with only one kind of particles denoted by A in which the elementary processes are diffusion, coagulation and decoagulation. This model is integrable and allows the occupation probability $<n_i>(t)$ of site i to be computed analytically. A detailed analysis for *periodic boundary conditions* has been given in our previous article [1] (hereafter referred to as I), where we focused our attention on the finite-size scaling properties of the concentration:

$$c(L,t) \;=\; \frac{1}{L}\sum_{i=1}^{L} <n_i>(t) \tag{1.1}$$

in the scaling limit $L \to \infty$, $t \to \infty$ keeping the scaling variable $z = \frac{4Dt}{L^2}$ fixed. We computed the corresponding scaling functions exactly and observed that they do not depend on the initial conditions.

In this paper we consider the same model with *open boundary conditions*. In particular we want to understand how the boundary conditions modify the finite-size scaling properties of the concentration $c(L,t)$.

Let us first describe the model and outline the method which allows us to compute the concentration. The model is defined by three elementary processes:

• diffusion	rate D	$\emptyset + A$	$\leftrightarrow$	$A + \emptyset$	
• coagulation	rate c	$A + A$	$\to$	A	(1.2)
• decoagulation	rate a	A	$\to$	$A + A$	

where A and $\emptyset$ denote an occupied and an empty site, respectively. The empty interval approach, which we will use to calculate the concentration, requires that coagulation and diffusion take place with equal rates. Therefore we have to choose $c = D$. Furthermore it is convenient to fix the time scale so that $D = 1$. The system is now controlled only by one parameter, namely the decoagulation rate a. Since all rates are chosen to be left-right symmetric the model is invariant under space reflection. In paper I we summarized how the master equation of the reaction-diffusion system defined by (1.2) can be mapped onto a one-dimensional quantum chain [2]. In this formulation the time evolution of the model is described by the euclidean Schrödinger equation:

$$\frac{\partial}{\partial t}|P\rangle \;=\; -\tilde{H}|P\rangle \tag{1.3}$$

where the Hamiltonian $\tilde{H}$ is given by:

$$\tilde{H} \;=\; \sum_{i=1}^{L-1} \tilde{H}_i \tag{1.4}$$

and:

$$\begin{aligned} \tilde{H}_i \;=\;& +2E_i^{11}\otimes E_{i+1}^{11} + (1+a)(E_i^{00}\otimes E_{i+1}^{11} + E_i^{11}\otimes E_{i+1}^{00}) \\ & -(E_i^{01}\otimes E_{i+1}^{10} + E_i^{10}\otimes E_{i+1}^{01} + E_i^{01}\otimes E_{i+1}^{11} + E_i^{11}\otimes E_{i+1}^{01}) \\ & -a(E_i^{10}\otimes E_{i+1}^{11} + E_i^{11}\otimes E_{i+1}^{10})\,. \end{aligned} \tag{1.5}$$

Here $E_i^{\alpha\beta}$ are 2×2 matrices defined by $(E_i^{\alpha,\beta})_{k,l} = \delta_k^\alpha \delta_l^\beta$ acting on the i^{th} site. Notice that open boundary conditions are already implemented in Eq. (1.4). Our aim is to compute the mean value of the concentration:

$$c(L,t) \;=\; \frac{1}{L}\sum_{i=1}^{L} <n_i>(t) \;=\; \frac{1}{L}\sum_{i=1}^{L}\langle 0|E_i^{11}\,\exp(-\tilde{H}t)|P_0\rangle \tag{1.6}$$

for an arbitrary initial state $|P_0\rangle$ (for notations we refer to paper I).

In our first paper we have shown that for $a \neq 0$ the Hamiltonian $\tilde{H}$ with periodic boundary conditions can be mapped onto the well-known anisotropic XY-chain with periodic boundary conditions. Since the corresponding similarity transformation is local, it also applies to the case of open boundary conditions. One obtains the Hamiltonian:

$$H^{XY} \;=\; -\frac{\eta}{2}\sum_{i=1}^{L-1}\Big(\eta\,\sigma_i^x\sigma_{i+1}^x \;+\; \eta^{-1}\sigma_i^y\sigma_{i+1}^y \;+\; \sigma_i^z \;+\; \sigma_{i+1}^z \;-\; \eta - \eta^{-1}\Big) \tag{1.7}$$

where:

$$\eta \;=\; \sqrt{1+a} \tag{1.8}$$

is a real parameter. Notice that although the original system (1.4) is defined with open boundary conditions, in Eq. (1.7) we do *not* obtain a quantum chain with free boundaries since there are additional fields $\frac{2}{\eta}(\sigma_1^z + \sigma_L^z)$ at the ends of the chain. The XY-chain is integrable, i.e. it can be diagonalized exactly in terms of free fermions, which allows to write the Hamiltonian (1.7) in the diagonal form [3]:

$$H^{XY} \;=\; \sum_{k=0}^{L-1}\Lambda_k\, a_k^\dagger a_k\,, \tag{1.9}$$

where $a_k^\dagger$ and a_k are fermionic operators:

$$\{a_k^\dagger, a_l\} \;=\; \delta_{k,l}\,. \tag{1.10}$$

The Λ_k are the corresponding fermionic excitation energies and are given by:

$$\Lambda_0 \;=\; 0\,, \tag{1.11}$$

$$\Lambda_k \;=\; \eta\left(\eta + \eta^{-1} - 2\cos\frac{\pi k}{L}\right), \qquad k = 1,\ldots,L-1\,. \tag{1.12}$$

The excitation with vanishing energy (1.11) for arbitrary η is related to a hidden quantum group symmetry [4] and implies the levels of the spectrum to be at least two-fold degenerated. The second equation (1.12) is just the dispersion relation of the XY-chain and we observe that the system is massless for $\eta = 1$ ($a = 0$). Taking all combinations of the excitation energies Λ_k into account, one can construct the spectrum of H^{XY} and therewith the spectrum of $\tilde{H}$.

One way to compute the concentration $c(L,t)$ would be to diagonalize $\tilde{H}$ directly. This turns out to be very complicated since it is not known in advance which of the eigenvectors enter the expression for the concentration and thus all of them have to be calculated. Therefore we prefer a different approach based on so-called empty intervals probabilities instead of spin configurations [5, 6] (for a compact summary we refer to paper I, the most general formulation of this approach can be found in [7]). The time evolution of the probability $\Omega(j,n,t)$ of finding

an empty interval of length n extending from site $j+1-\frac{n}{2}$ to site $j+\frac{n}{2}$ is described by a closed system of linear differential equations. Since $1-\Omega(j-\frac{1}{2},1,t)$ is just the probability to find the $j^{\rm th}$ site occupied the concentration $c(L,t)$ is simply given by:

$$c(L,t) \;=\; \frac{1}{L}\sum_{j=1}^{L} <n_j>(t) \;=\; \frac{1}{L}\sum_{j=1}^{L}\Big(1-\Omega(j-\frac{1}{2},1,t)\Big)\,. \tag{1.13}$$

A detailed derivation of this formalism can be found in paper I. Here we present a modified version of the differential equations for open boundary conditions. If the interval does not touch the boundaries we have:

$$\begin{aligned}\frac{\partial\Omega(j,n,t)}{\partial t} \;&=\; \eta^2\Big(\Omega(j-\frac{1}{2},n+1,t)+\Omega(j+\frac{1}{2},n+1,t)\Big) \\ &\quad+\Omega(j-\frac{1}{2},n-1,t)+\Omega(j+\frac{1}{2},n-1,t)-2\,(\eta^2+1)\,\Omega(j,n,t)\,,\end{aligned} \tag{1.14}$$

where $\frac{n}{2}<j<L-\frac{n}{2}$ and $n=1,\cdots,L-1$. If on the other hand the interval touches the boundaries one obtains the 'boundary equations':

$$\begin{aligned}\frac{\partial\Omega(\frac{n}{2},n,t)}{\partial t} \;&=\; \eta^2\Omega(\frac{n+1}{2},n+1,t) \\ &\quad+\Omega(\frac{n-1}{2},n-1,t)-(\eta^2+1)\,\Omega(\frac{n}{2},n,t)\,,\end{aligned} \tag{1.15}$$

$$\begin{aligned}\frac{\partial\Omega(L-\frac{n}{2},n,t)}{\partial t} \;&=\; \eta^2\Omega(L-\frac{n+1}{2},n+1,t) \\ &\quad+\Omega(L-\frac{n-1}{2},n-1,t)-(\eta^2+1)\,\Omega(L-\frac{n}{2},n,t)\,,\end{aligned} \tag{1.16}$$

$$\frac{\partial\Omega(\frac{L}{2},L,t)}{\partial t} \;=\; 0\,. \tag{1.17}$$

As in paper I in all equations we use the convention:

$$\Omega(j,0,t)=1\,. \tag{1.18}$$

Therefore this system of equations is inhomogeneous. A particular solution is obviously given by:

$$\Omega(j,n,t) \;=\; 1 \tag{1.19}$$

corresponding to an empty lattice. In this notation the space reflection is described by the map:

$$P\;:\;(j,n)\mapsto(L-j,n)\,. \tag{1.20}$$

As one can easily check the system of differential equations (1.14)-(1.17) is invariant under P. Notice that, in opposition to the case of periodic boundary conditions where the Fourier transformed system has only $L-1$ degrees of freedom, this system has $L(L+1)/2$ degrees of freedom. It grows quadratically with lattice length L and thus it is more difficult to solve. The central mathematical aspect of this paper is the exact solution of this problem.

Because of the reduced number of degrees of freedom compared to the original physical system the set of differential equations (1.14)-(1.17) can only cover a part of the full dynamics

of the Hamiltonian (1.4). As we will see in Sec. 2 this part corresponds just to those states of the XY chain with only one or two excited fermions. The advantage of the empty interval formalism is that $c(L,t)$ can be computed easily via Eq. (1.13).

This article is organized as follows. In Sec. 2 we solve the system of differential equations (1.14)-(1.17). We then derive exact expressions for $c(L,t)$ for special initial conditions in Sec. 3 and analyse the corresponding finite-size scaling properties. Finally we summarize our results.

2 Solution of the System of Differential Equations

In this section we solve the system of differential equations (1.14)-(1.17). For this purpose we first determine the complete set of solutions $\phi_\Lambda(j,n,t)$ of the homogeneous eigenvalue problem:

$$\frac{\partial}{\partial t}\phi_\Lambda(j,n,t) \;=\; -\Lambda\,\phi_\Lambda(j,n,t)\,, \tag{2.1}$$

where Eq. (1.18) has to be replaced by:

$$\phi_\Lambda(j,0,t) = 0 \tag{2.2}$$

in order to impose homogeneous boundary conditions. It will be convenient to introduce the notations:

$$x = j + \frac{n}{2}\,, \qquad\qquad y = j - \frac{n}{2} \tag{2.3}$$

where x and y take the values $0 \le y \le x \le L$. In this notation the space reflection reads:

$$P \;:\; (x,y) \mapsto (L-y, L-x)\;. \tag{2.4}$$

For $0 < y < x < L$ the system of differential equations (1.14)-(1.17) now has the form:

$$\begin{aligned}\frac{\partial\phi(x,y,t)}{\partial t} \;&=\; \eta^2\left(\phi(x+1,y,t)+\phi(x,y-1,t)\right) \\ &\quad + \phi(x-1,y,t)+\phi(x,y+1,t) - 2(\eta^2+1)\,\phi(x,y,t)\,,\end{aligned} \tag{2.5}$$

$$\frac{\partial\phi(x,0,t)}{\partial t} \;=\; \eta^2\phi(x+1,0,t) + \phi(x-1,0,t) - (\eta^2+1)\,\phi(x,0,t)\;, \tag{2.6}$$

$$\frac{\partial\phi(L,y,t)}{\partial t} \;=\; \eta^2\phi(L,y-1,t) + \phi(L,y+1,t) - (\eta^2+1)\,\phi(L,y,t)\;, \tag{2.7}$$

$$\frac{\partial\phi(L,0,t)}{\partial t} \;=\; 0\;. \tag{2.8}$$

For $0 \le x = y \le L$ we have:

$$\phi(x,x,t) = 0\;, \tag{2.9}$$

or:

$$\phi(x,x,t) = 1 \tag{2.10}$$

if we choose the system to be homogeneous or inhomogeneous, respectively. For easy reference we illustrated the organization of the complete system for $L = 6$ sites in Fig. 1. Here the

$L(L+1)/2$ boxes represent the degrees of freedom $\phi(x,y)$. The number in each box denotes the strength of the diagonal contribution in the differential equations, where $d = -(2+a) = -(1+\eta^2)$, while the arrows denote the flow of probability to the neighbours with respect to the couplings

$$\begin{aligned} \rightarrow, \downarrow: &\qquad 1 \\ \leftarrow, \uparrow: &\qquad 1 + a = \eta^2 \,. \end{aligned}$$

The zeros on the hypotenuse $x = y$ represent the contributions from the inhomogenous part of the system. Since we consider only the homogenous equation due to Eq. (2.9) these terms have to be neglegted throughout this section.

Before calculating the solutions of the eigenvalue problem of Eq. (2.1) we give a short description how to proceed. Looking at Fig. 1 we find that the boxes on the short sides of the triangle form a decoupled $(2L-1)$-dimensional subsystem of differential equations. As a consequence we expect two kinds of solutions:

- The first kind is obtained by solving the subsystem separately. Since each solution imposes inhomogeneous Dirichlet boundary conditions it can be extended uniquely to the interior of the triangle. This procedure yields a set of $2L-1$ solutions of Eq. (2.1) forming a complete set of eigenfunctions for the short sides of the triangle.

- The second kind of solutions is now calculated using the completeness of the first kind solutions. They are forced to vanish on the boundary and therefore to obey homogeneous Dirichlet boundary conditions.

Let us now study the solution of (2.1) in more detail. For the moment we choose $\eta = 1$ (see Eq. (1.8)). Then the differential equations acting on the short sides of the triangle are:

$$D_x^2\, \phi_\Lambda(x,0) = -\Lambda\, \phi_\Lambda(x,0), \tag{2.11}$$

$$D_y^2\, \phi_\Lambda(L,y) = -\Lambda\, \phi_\Lambda(L,y)\,, \tag{2.12}$$

where $x, y = 1, \cdots, L-1$. Here D_x^2 and D_y^2 are discrete second derivative operators in x and y direction, respectively. D_x^2 for example is defined by $D_x^2\phi(x,y) = \phi(x+1,y) + \phi(x-1,y) - 2\phi(x,y)$.

The probability for an empty lattice $\phi_\Lambda(L,0)$ decouples completely and remains constant in time. Thus $\phi_\Lambda(L,0)$ takes nonzero values only if $\Lambda = 0$. In this case the second derivative of $\phi_{\Lambda=0}$ vanishes and ϕ_0 becomes a linear function of x and y, namely $\phi_0(x,y) \sim x - y$ due to Eq. (2.9). For $\Lambda \neq 0$ the condition $\phi_\Lambda(L,0) = 0$ gives an additional constraint which determines the solutions of Eqs. (2.11) and (2.12) to be simple oscillations:

$$\phi(x,0) \sim \sin\frac{\pi k x}{L}\,, \quad \phi(L,y) \sim \sin\frac{\pi k y}{L}\,, \tag{2.13}$$

$$\Lambda_k = 2\left(1 - \cos\frac{\pi k}{L}\right),$$

where $k = 1, \ldots, L-1$. The values of Λ give the spectrum of eigenvalues. Comparing it with the spectrum of the XY-chain (1.9) we recognize that it corresponds to one-fermion

excitations. For a given $\Lambda_k \neq 0$ every linear combination of the solutions of Eq. (2.13) solves Eqs. (2.11) and (2.12). Thus these eigenvalues are twofold degenerated. However, we can choose the functions ϕ_k to be eigenfunctions of the space reflection P (see (2.4), too. It will be convenient to introduce the notation $P\phi_k^\pm = \pm(-1)^k\phi_k^\pm$. So far we have determined the required $2L-1$ solutions on the short sides of the triangle which still have to be extended to the interior. Here the differential equations act according to $(D_x^2 + D_y^2)\phi = -\Lambda\phi$ where the operator on the left side is just the discrete Laplacian. The solutions are given below in Eqs. (2.15) and (2.16).

Now we turn to the calculation of the remaining $\frac{(L-1)(L-2)}{2}$ solutions of the interior of the triangle. These solutions are plane waves (2.17) vanishing on the boundary of the triangle. The corresponding eigenvalues $\Lambda = \Lambda_k + \Lambda_l$ are identified as two-fermion excitations of the XY-chain.

Summing up all results we have three types of solutions:

- The stationary solution:
$$\phi_0(x,y) \;=\; \frac{x-y}{L}\;. \tag{2.14}$$

- One-fermion excitations ($k = 1, \ldots, L-1$):
$$\phi_k^+(x,y) \;=\; \frac{1}{\sqrt{L}}\Big(\sin\frac{\pi k}{L}x - \sin\frac{\pi k}{L}y\Big)\;, \tag{2.15}$$
$$\phi_k^-(x,y) \;=\; \frac{1}{\sqrt{L}}\Big((1-\frac{2y}{L})\sin\frac{\pi k}{L}x - (1-\frac{2x}{L})\sin\frac{\pi k}{L}y\Big)\;. \tag{2.16}$$

- Two-fermion excitations ($k, l = 1, \ldots, L-1; k < l$):
$$\Phi_{kl}(x,y) \;=\; \frac{2}{L}\Big(\sin\frac{\pi k}{L}x\,\sin\frac{\pi l}{L}y - \sin\frac{\pi l}{L}x\,\sin\frac{\pi k}{L}y\Big)\;. \tag{2.17}$$

This is the complete set of $L(L+1)/2$ solutions of the homogeneous system. For $\eta \neq 1$ we obtain deformations of these solutions. In order to avoid too much details, we only want to present our results:

- The stationary solution:
$$\phi_0(x,y) \;=\; \frac{1-\eta^{2(y-x)}}{1-\eta^{-2L}} \tag{2.18}$$
with eigenvalue $\Lambda = 0$ and parity $P = +1$.

- One-fermion excitations ($k = 1, \ldots, L-1$):
$$\phi_k^\pm(x,y) \;=\; \frac{1}{\sqrt{L}}\frac{\eta^{y-x}}{1\pm\eta^L}\Big((\eta^y \pm \eta^{L-y})\sin\frac{\pi k}{L}x - (\eta^x \pm \eta^{L-x})\sin\frac{\pi k}{L}y\Big) \tag{2.19}$$
with eigenvalue $\Lambda_k = \eta(\eta + \eta^{-1} - 2\cos\frac{\pi k}{L})$ (see Eq. (1.12)) and parity $P = \pm(-1)^k$.

- Two-fermion excitations ($k, l = 1, \ldots, L-1; k < l$):

$$\Phi_{kl}(x,y) \;=\; \frac{2}{L}\eta^{y-x}\Big(\sin\frac{\pi k}{L}x\,\sin\frac{\pi l}{L}y - \sin\frac{\pi l}{L}x\,\sin\frac{\pi k}{L}y\Big) \tag{2.20}$$

with eigenvalues $\Lambda_{kl} = \eta(2\eta + 2\eta^{-1} - 2\cos\frac{\pi k}{L} - 2\cos\frac{\pi l}{L})$ and parity $P = (-1)^{k+l+1}$.

It is easy to check that these solutions reduce to Eqs. (2.14)-(2.17) in the limit $\eta \to 1$.

Let us now study the orthogonality relations of the different types of solutions. The functions $\phi_k^{\pm}$, $k \neq 0$ form a complete system of eigenfunctions on the short sides of the triangle except the point $(L, 0)$. The corresponding scalar product denoted by $\langle\,|\,\rangle_{\text{boundary}}$ takes only these points into account. For arbitrary functions f, g we define:

$$\langle f \,|\, g\rangle_{\text{boundary}} = \sum_{x=1}^{L-1} \eta^{2x} f(x,0)g(x,0) + \sum_{y=1}^{L-1} \eta^{2(L-y)} f(L,y)g(L,y)\,. \tag{2.21}$$

The solutions (2.19) are normalized in such a way that:

$$\langle \phi_k^{\alpha} \,|\, \phi_{k'}^{\beta}\rangle_{\text{boundary}} = \delta_{kk'}\delta_{\alpha\beta} \tag{2.22}$$

where $k, k' = 1, \ldots, L-1$ and $\alpha, \beta = \pm$. For the functions Φ_{kl} (2.20) we define a scalar product in the interior of the triangle:

$$\langle f \,|\, g\rangle_{\text{bulk}} = \sum_{x=1}^{L-1}\sum_{y=1}^{x-1} \eta^{2(x-y)} f(x,y)g(x,y)\,. \tag{2.23}$$

Then the functions Φ_{kl} (2.20) obey the relation:

$$\langle \Phi_{kl} \,|\, \Phi_{k'l'}\rangle_{\text{bulk}} = \delta_{kk'}\delta_{ll'}\,. \tag{2.24}$$

These relations are independent of the value of η. Unfortunately the solutions $\phi_k^{\pm}$ take nonzero values in the interior of the triangle. Therefore the scalar product $\langle \Phi_{kl} \,|\, \phi_{k'}^{\pm}\rangle_{\text{bulk}}$ is not equal to zero. These projections have to be taken into account if one expands an arbitrary function $\Omega(x, y)$ in terms of the eigenfunctions as we will do in the next section.

3 Finite-Size Scaling of the Concentration

In this section we use the complete set of eigenfunctions found in Sec. 2 in order to calculate the time evolution of the concentration for an initially fully occupied lattice and an arbitrary value of η. In the case of $\eta = 1$ the finite-size scaling limit is computed and compared with the corresponding result for periodic boundary conditions.

Before calculating the concentration for special initial conditions we consider the general case. Let $\Omega_0(x, y)$ be an arbitrary initial choice of empty interval probabilities satisfying condition (1.18). The time evolution then takes the form:

$$\Omega(x,y,t) = 1 + \omega_0\phi_0(x,y) + \sum_{k=1}^{L-1}\sum_{\alpha=\pm} \omega_k^{\alpha}\phi_k^{\alpha}(x,y)e^{-\Lambda_k t} + \sum_{k=1}^{L-2}\sum_{l=k+1}^{L-1} \omega_{kl}\Phi_{kl}(x,y)e^{-(\Lambda_k+\Lambda_l)t} \tag{3.1}$$

where the constant 1-function is just the particular solution (1.19) and Λ_k is defined in Eq. (1.12). The coefficients ω_0, $\omega_k^{\pm}$ and ω_{kl} are obtained by expanding $\Omega_0(x,y)$ in terms of the eigenfunctions (2.18)-(2.20). Therefore we first consider Eq. (3.1) for $t=0$ at the point $(L,0)$. Since all eigenfunctions except ϕ_0 vanish at this point we have:

$$\omega_0 = \Omega_0(L,0) - 1 \; . \tag{3.2}$$

Then we consider the short sides of the triangle, where the eigenfunctions Φ_{kl} vanish. Here the coefficients $\omega_k^{\pm}$ can be obtained using the relation (2.22):

$$\omega_k^{\pm} = \langle \phi_k^{\pm} \,|\, \Omega_0 - 1 - \omega_0\phi_0 \rangle_{\text{boundary}} \; . \tag{3.3}$$

Finally we calculate the remaining coefficients ω_{kl} with the help of Eq. (2.24):

$$\omega_{kl} = \langle \Phi_{kl} \,|\, \Omega_0 - 1 - \omega_0\phi_0 \rangle_{\text{bulk}} - \sum_{k'=1}^{L-1} \sum_{\alpha=\pm} \omega_{k'}^{\alpha} \langle \Phi_{kl} \,|\, \phi_{k'}^{\alpha} \rangle_{\text{bulk}} \; . \tag{3.4}$$

We now apply this general procedure to the case of an uncorrelated initial state where the occupation probability p is equal for all sites (see paper I). Then we have:

$$\Omega_0(x,y) = (1-p)^{x-y} \; . \tag{3.5}$$

Straightforward but rather laborious calculations show that the concentration is given by:

$$\begin{aligned}
c(t,L) \;=\; & \frac{1-\eta^{-2}}{1-\eta^{-2L}}(1-(1-p)^L) \\
& + \frac{4\,(1-\eta^{-2})}{L^2(\eta^L-\eta^{-L})} \sum_{k=1}^{L-1} (1-(1-p)^L\eta^L(-1)^k)(\eta^L+\eta^{-L}-2(-1)^k) \\
& \qquad \times \frac{\sin^2(\frac{\pi k}{L})}{\Lambda_k}\Big(\frac{1}{\Lambda_k}-\frac{1}{\tilde\Lambda_k}\Big)\exp\left(-\Lambda_k t\right) \\
& + \frac{8}{L^3\eta} \sum_{k=1}^{L-1} \sum_{\substack{l=k+1 \\ k+l \text{ odd}}}^{L-1} \frac{\sin^2\frac{\pi k}{L}\,\sin^2\frac{\pi l}{L}}{\cos\frac{\pi k}{L}-\cos\frac{\pi l}{L}} \Big[\frac{1}{\cos\frac{\pi k}{L}-\cos\frac{\pi l}{L}} \Big(\frac{1}{\Lambda_k}+\frac{1}{\Lambda_l}-\frac{1}{\tilde\Lambda_k}-\frac{1}{\tilde\Lambda_l} \Big) \\
& \qquad + 2\Big(\frac{1}{\Lambda_k}-\frac{1}{\tilde\Lambda_k}\Big)\Big(\frac{1}{\Lambda_l}-\frac{1}{\tilde\Lambda_l}\Big)\eta^L(1-p)^L(-1)^k \\
& \qquad - \frac{2}{\Lambda_k\tilde\Lambda_l} + \frac{2}{\Lambda_l\tilde\Lambda_k} \Big] \; \exp\left(-(\Lambda_k+\Lambda_l)t\right) \; ,
\end{aligned} \tag{3.6}$$

where $\tilde\Lambda_k$ is defined by:

$$\tilde\Lambda_k \;=\; \eta\Big((1-p)\eta + (1-p)^{-1}\eta^{-1} - 2\cos\frac{\pi k}{L}\Big) \; . \tag{3.7}$$

Now we consider the finite-size scaling limit of the concentration. As pointed out in paper I we assume that in the finite-size scaling regime $L\to\infty, t\to\infty$, $z=\frac{4t}{L^2}$ fixed the concentration behaves like:

$$c(z,L) = L^x[F_0(z) + L^{-y}F(z) + \cdots] \; . \tag{3.8}$$

In this formula $F_0(z)$ denotes the scaling function and x the scaling exponent. $L^y F(z)$ is the leading correction term. The functions $F_0(z)$ and $F(z)$ are supposed to depend only on z. Since the finite-size scaling hypothesis is only valid for critical systems corresponding to massless quantum chains we have to restrict ourselves to the case $\eta = 1$. In this case the concentration takes the form:

$$\begin{aligned} c(t,L) &= \frac{1-(1-p)^L}{L} \\ &+ \frac{4}{L^3}\sum_{k=0}^{L-1}\sum_{\substack{l=1\\ k+l \text{ odd}}}^{L-1} \frac{\sin^2\frac{\pi k}{L}\,\sin^2\frac{\pi l}{L}}{\cos\frac{\pi k}{L}-\cos\frac{\pi l}{L}}\Big[\frac{1}{\cos\frac{\pi k}{L}-\cos\frac{\pi l}{L}}\Big(\frac{1}{\Lambda_k}+\frac{1}{\Lambda_l}-\frac{1}{\tilde\Lambda_k}-\frac{1}{\tilde\Lambda_l}\Big) \\ &\qquad + 2\Big(\frac{1}{\Lambda_k}-\frac{1}{\tilde\Lambda_k}\Big)\Big(\frac{1}{\Lambda_l}-\frac{1}{\tilde\Lambda_l}\Big)(1-p)^L(-1)^k \\ &\qquad -\frac{2}{\Lambda_k\tilde\Lambda_l}+\frac{2}{\Lambda_l\tilde\Lambda_k}\Big]\ \exp\left(-(\Lambda_k+\Lambda_l)t\right)\,. \end{aligned} \tag{3.9}$$

Performing now the finite-size scaling limit we get for the functions $F_0(z)$ and $F(z)$:

$$F_0(z) = 1+\frac{16}{\pi^2}\sum_{k=0}^{\infty}\sum_{\substack{l=1\\ k+l \text{ odd}}}^{\infty}\frac{k^2+l^2}{(k^2-l^2)^2}\exp\Big(-\frac{z\pi^2}{4}(k^2+l^2)\Big)\,, \tag{3.10}$$

$$\begin{aligned} F(z) &= \sum_{k=0}^{\infty}\sum_{\substack{l=1\\ k+l \text{ odd}}}^{\infty}\Big(\frac{z}{3}\pi^2\frac{(k^2+l^2)(k^4+l^4)}{(k^2-l^2)^2}-\frac{8}{3}\frac{(1+6\frac{1-p}{p^2})(k^4+l^4)+k^2l^2}{(k^2-l^2)^2}\Big) \\ &\qquad \times\exp\Big(-\frac{z\pi^2}{4}(k^2+l^2)\Big) \end{aligned} \tag{3.11}$$

and for the exponents $x,\ y$:

$$x=-1, \qquad y=2\,. \tag{3.12}$$

The functions F_0 and F can be written in a simpler form by rewriting the sums in Eqs. (3.10) and (3.11) in terms of $\mu=\frac{k+l-1}{2}$ and $\nu=\frac{k-l-1}{2}$:

$$F_0(z) = 1-\frac{1}{2}g_0(z)\,g_1(z)\,, \tag{3.13}$$

$$\begin{aligned} F(z) &= -\frac{7z}{12}g_1(z)g_2(z)-\frac{z}{12}g_0(z)g_3(z)-\frac{1}{12}\Big(g_0(z)g_2(z)-\Big(g_1(z)\Big)^2\Big) \\ &\quad -(1+6\frac{1-p}{p^2})\Big(\frac{1}{6}g_0(z)g_2(z)+\frac{1}{2}\Big(g_1(z)\Big)^2\Big) \end{aligned} \tag{3.14}$$

where the functions $g_i(z)$ are defined by:

$$g_0(z) = \sum_{\mu=-\infty}^{\infty}\frac{-2}{\pi^2(\mu+\frac{1}{2})^2}\exp\Big(-\frac{z\pi^2}{2}(\mu+\frac{1}{2})^2\Big)\,, \tag{3.15}$$

$$g_i(z) = \frac{\partial^i}{\partial z^i}g_0(z)\,,\ i=1,\cdots,3\,. \tag{3.16}$$

Especially we have the identity:

$$g_1(z) = \theta_2\Big(0, \frac{i\pi z}{2}\Big) \tag{3.17}$$

where $\theta_2(u,\tau)$ is a Jacobi-Theta function. Now we are able to compare the finite-size scaling behaviour for open and periodic boundary conditions. In both cases we find the scaling exponent $x = -1$ and the correction exponent $y = 2$. Thus the critical exponents are not influenced by the boundary conditions. The scaling function and the correction function on the other hand are different as can be seen in Fig. 2 and Fig. 3. However we find that in both cases the scaling functions and the correction functions are related to Jacobi-Theta functions. As in the case of periodic boundary conditions we observe that the scaling function (3.10) is independent of the initial probability p whereas the correction function (3.11) is not.

4 Conclusions

Based on the empty interval probability approach we solved the coagulation-decoagulation model defined on a lattice of L sites with open boundary conditions. In contrast to ordinary mean-field calculations our results take the microscopic fluctuations of the system into account. We computed the concentration $c(L,t)$ exactly and investigated its finite-size scaling properties. Our aim was to compare the results with those of our previous paper [1], where periodic boundary conditions have been considered.

Mathematically the time evolution of the empty interval probabilities is described by a system of $L(L+1)/2$ linear differential equations (in opposition to only $L-1$ equations in the case of periodic boundary conditions). It is the first time that such a system has been solved in the theory of reaction-diffusion processes, and we sketched the general method how to find the solutions. We obtained three types of solutions wich can be interpreted as states with none, one and two fermions in an excited state.

We used the expression for $c(L,t)$ to compute the finite-size scaling expansion of the concentration and compared the result with the case of periodic boundary conditions. It turned out that one obtains the same type of expansion (with the same powers in $1/L$). As in the periodic case we found that the scaling function is independend of uncorrelated homogeneous initial conditions. However, they are different for open and periodic boundary conditions. On the other hand the correction function is influenced by the initial condition similar to the periodic case. In this paper we only investigated homogeneous uncorrelated initial conditions. Initial states with small clusters are studied numerically. The results are presented in [8]. It turns out that the scaling function remains unchanged even for that kind of initial conditions.

Using the empty interval approach we can compute the local concentration $c_j(t)$. As mentioned in the introduction, this formalism does not cover the full dynamical space of the physical system. In particular it is impossible to compute correlations between concentrations located at distinct points. For this reason we want to outline a possible generalization. An empty interval can be understood as a two-point object. Therefore it is natural to consider also generalized $2n$-point objects consisting of n separated empty intervals. These objects are also expected to be described by a set of linear differential equations as well. In particular they are nothing but n-point correlation functions of the occupation number if we choose the

lengths of all intervals to be equal to one (similar to Eq. (1.13)). Of course we expect a higher number of fermionic excitations to be involved.

References

[1] K. Krebs, M. Pfannmüller, B. Wehefritz, *Finite-Size Scaling Studies in Reaction-Diffusion Systems, Part I: Periodic boundary conditions, University of Bonn preprint* BONN HE-93-51 (1993).

[2] F.C. Alcaraz, M. Droz, M. Henkel and V. Rittenberg, *Reaction-Diffusion Processes, Critical Dynamics and Quantum Chains*, *University of Genève preprint UGVA-DPT* 1992/12-799, to appear in *Ann. Phys.* (1994).

[3] E. Lieb, T. Schultz and D. Mattis, *Ann. Phys.* (New York) **16**:407 (1961).

[4] H. Hinrichsen and V. Rittenberg, *Phys. Lett.* **B 275**:350 (1992).

[5] D. ben-Avraham, M. A. Burschka and C. R. Doering, *J. Stat. Phys.* **60**:695 (1990).

[6] C. R. Doering, M. A. Burschka and W. Horsthemke, *J. Stat. Phys.* **65**:953 (1991).

[7] I. Peschel, V. Rittenberg, U. Schultze, *Integrable quantum chains without Bethe Ansatz. Probabilistic methods*, *in preparation*.

[8] K. Krebs, M. Pfannmüller, H. Simon and B. Wehefritz, *Finite-Size Scaling Studies in Reaction-Diffusion Systems, Part III: Numerical Methods, University of Bonn preprint* BONN HE-94-02 (1994).

List of Figures

Fig. 1: Structure of the system of differential equations for $L = 6$ sites. The figure is explained in the text.

Fig. 2: Scaling functions for open and periodic boundary conditions.

Fig. 3: Correction functions for open and periodic boundary conditions for initial occupation probability $p = 1$.

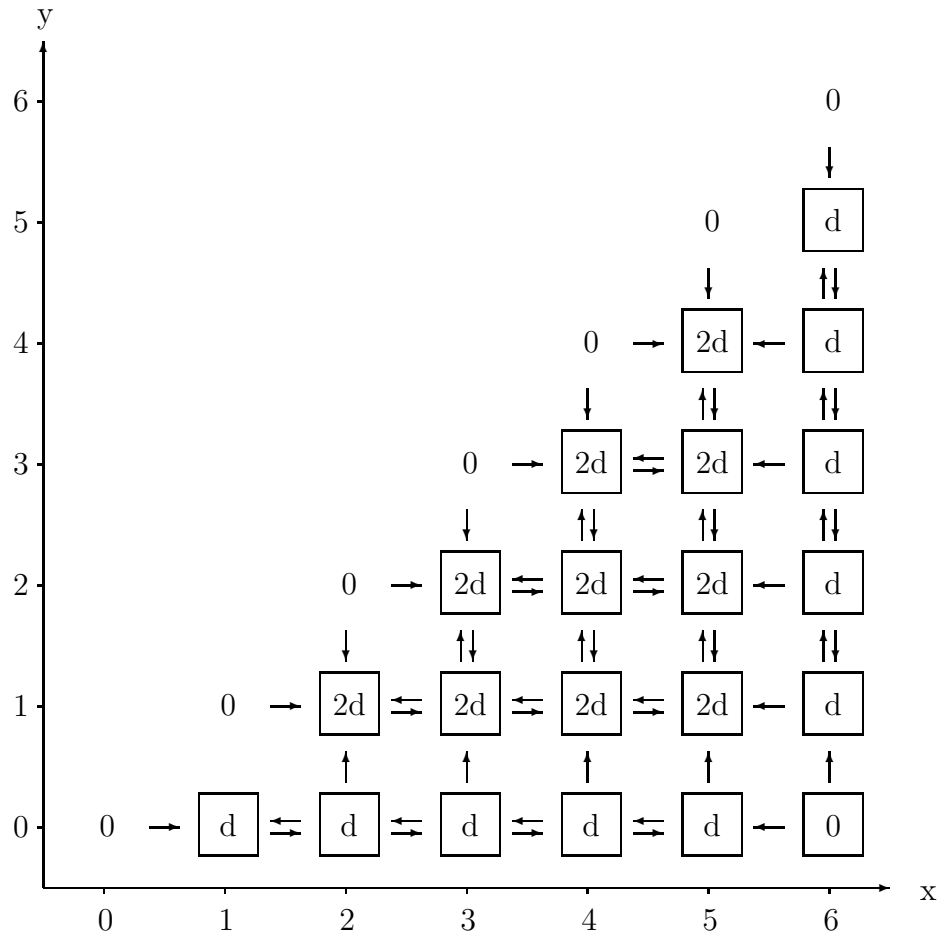

Figure 1: Structure of the system of differential equations for $L = 6$ sites. The figure is explained in the text.

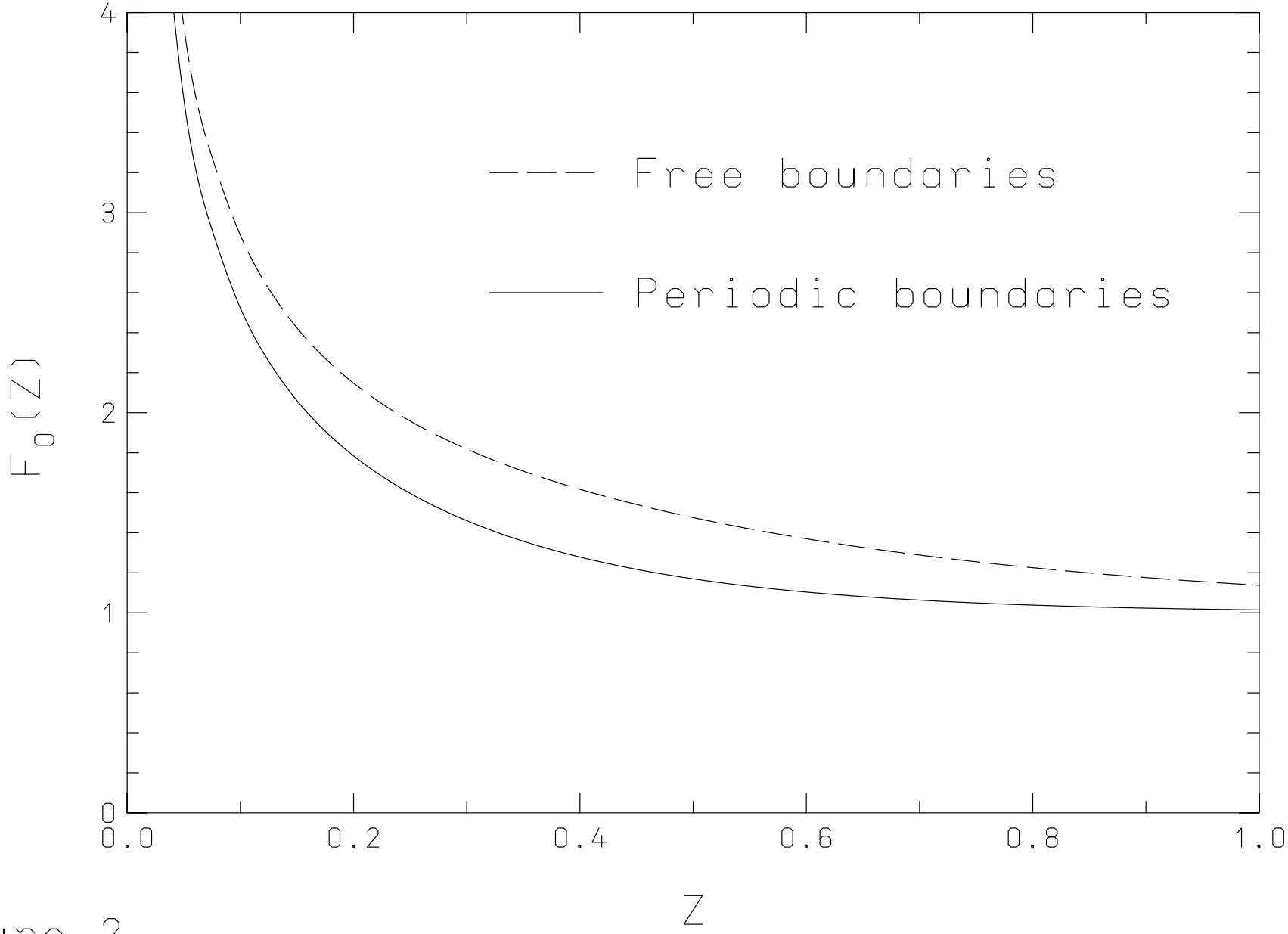
Free boundaries
Periodic boundaries
$F_o(Z)$
Z
0
1
2
3
4
0.0
0.2
0.4
0.6
0.8
1.0

Figure 2

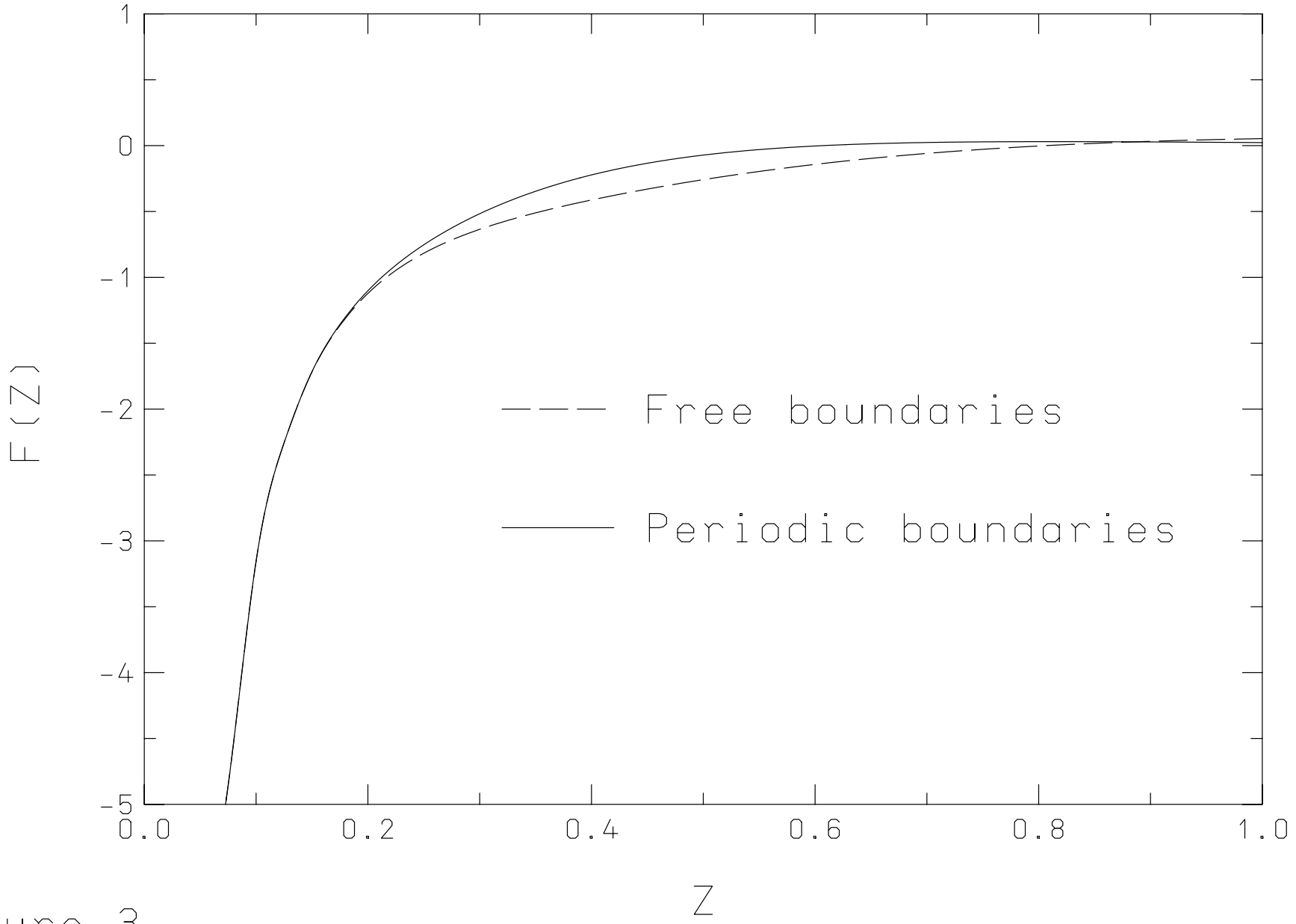
1
0
-1
-2
-3
-4
-5
F(Z)
0.0
0.2
0.4
0.6
0.8
1.0
Z
Free boundaries
Periodic boundaries

Figure 3